Ping Qu
Lei Zhang
Jin Sheng
Jianping Lei
Huangxian Ju

Key Laboratory of Analytical Chemistry for Life Science (Ministry of Education of China), Department of Chemistry, Nanjing University, Nanjing, P. R. China

Received December 9, 2010
Revised March 7, 2011
Accepted March 7, 2011

Research Article

Convenient enantioseparation by monolithic imprinted capillary clamped in a chip with electrochemical detection

A microchip integrated with a monolithic imprinted capillary has been manufactured for performing the chip-based capillary electrochromatographic enantioseparation. The microporous monolith anchored on the inner wall of the microchannel was prepared by in situ chemical copolymerization, and characterized with scanning electron microscopy, IR spectroscopy, and solid-state UV–vis spectroscopy. The monolithic network with high porosity gave a large surface area, good permeability, low mass-transfer resistance, and thus high separation efficiency. A portable microchip was conveniently constructed by integrating an imprinted capillary with 5-cm length as the separation channel and a carbon fiber microdisk working electrode for amperometric detection. Using L-tyrosine (L-Tyr) as the template molecule, Tyr enantiomers could be baseline separated within 55 s under the optimized preparation and separation conditions. The linear ranges for online amperometric detection of both Tyr enantiomers were from 20 to 2400 μM. The microporous monolithic chip strategy exhibited excellent separation efficiency and promising analytical application in enantioseparation. It opens an avenue for high-throughput screening of chiral compounds.

Keywords:
Capillary electrochromatography / Enantioseparation / Microfluidics / Microporous monolith / Molecularly imprinted polymer DOI 10.1002/elps.201000655

1 Introduction

Molecularly imprinted polymers (MIPs), as a kind of polymer material with high selectivity, have been applied in different fields, such as separation media [1–10], catalysis [11], extraction [12, 13], biomimetic recognition [14–16], and sensing devices [17–19]. The use of MIPs as chiral stationary phases for the separation of enantiomers by high-performance liquid chromatography (HPLC) [20–22] and capillary electrochromatography (CEC) [4, 23–25] has attracted considerable interest. Recently, two studies have combined the prominent selectivity of MIPs with microchip electrochromatography (MCEC) for the rapid enantioseparation of chiral compound since MCEC has become an attractive approach for highly efficient separation [26, 27]. Although the enantioseparation has been achieved by open-tubular imprinting on microchannel wall, the separation performance is not satisfied due to the low column capacity of the microchannel [26]. Trapping MIP magnetic nanoparticles in the capillary as stationary phase can improve the column capacity, but it needs an external magnetic field, for example, a rare earth magnet [27].

Monolithic MIPs present a novel way for the preparation of stationary phases [28–30]. Compared with other methods for preparing MIPs as chiral stationary phases, including MIP particles packing [31, 32] and MIP particles as a mobile phase additive [2, 3], monolithic MIPs can be in situ prepared by a simple one-step method with high reproducibility, rapid mass transport, and easy tuning of the pore structure. This study used a new disposable stationary phase to minimize carryover problem compared with the suspended MIP particle-based CEC separations [33, 34]. In recent years, owing to their great porosity, good permeability, and high surface area, monolithic media have been extensively used for chromatographic separation in HPLC and CEC [35–37]. In this study, the microporous monolith was anchored on the inner wall of a chip microchannel, leading to a new technique to use a chip as a holder for a monolithic MIP-CEC capillary.

Correspondence: Professor Huangxian Ju, Key Laboratory of Analytical Chemistry for Life Science (Ministry of Education of China), Department of Chemistry, Nanjing University, Nanjing 210093, P. R. China
E-mail: hxju@nju.edu.cn
Fax: +86-25-83593593

Abbreviations: AM, acrylamide; **BR,** buffer reservoir; **DR,** detection reservoir; **EDMA,** ethylene glycol dimethacrylate; **FT-IR,** Fourier transform infrared; **L-Tyr,** L-tyrosine; **MCEC,** microchip electrochromatography; **MIPs,** molecularly imprinted polymers; **NIP,** nonimprinted polymer; **SEM,** scanning electron micrographs; **SR,** sample reservoir; **WE,** working electrode

Color Online: See the article online to view Figs. 1, 3, 4, 6, 7, 8 in colour.

Enantioselective separation of amino acids has been a topic with great attention because the ratio of D/L-amino acids in foodstuffs is an indicator of the quality and nutritional value [38] and D-amino acids are also the candidates of intrinsic physiologically active substance and the disease biomarkers in mammals [39, 40]. In view of the importance of trace D-Tyr in the evaluation of human health, this study selected racemic Tyr as the model enantiomers. The microporous monolithic imprinted capillary was prepared using acrylamide (AM) as the functional monomer and ethylene glycol dimethacrylate (EDMA) as the cross-linker by in situ thermal-initiated copolymerization technique. The resulting capillary as microfluidic channel could conveniently be fixed into a poly(dimethylsiloxane) (PDMS) substrate to construct a portable microchip (Fig. 1). Amperometric detection was selected due to the excellent electrochemical response of racemic Tyr at carbon fiber electrode and convenient integration of the electrode with the microchannel, which has been applied widely on the electrophoresis microchip [41–43]. With the imprinted microchannel and a home-made carbon fiber microdisk electrode on this microchip, baseline enantioseparation and amperometric detection of racemic Tyr were achieved within 55 s. The designed microchip with microporous monolithic imprinted microfluidic channel showed excellent separation efficiency and promising analytical application in rapid enantioseparation.

2 Materials and methods

2.1 Reagents

L-Tyrosine (L-Tyr), racemic Tyr, 3-(methacryloyloxy)propyltrimethoxysilane (γ-MPS), AM, and EDMA were all purchased from Alfa Aesar (Ward Hill, MA, USA). 2,2′-Azobisisobutyronitrile (AIBN) was obtained from Acros (Geel, Belgium). HPLC-grade acetonitrile (ACN) was supplied by Sigma-Aldrich (St. Louis, MO, USA). Isooctane was supplied by Shanghai Chemical Reagent (Shanghai, China). Quartz capillary with an inner diameter (id) of 25 μm and outer diameter (od) of 365 μm was purchased from Yongnian Optic Fiber Plant (Hebei, China). Sylgard 184 silicone elastomer and curing agent were purchased from Dow Corning (Midland, MI, USA). Both the mobile phase and the supporting electrolyte for MCEC separation and amperometric detection were a mixture of ACN and acetate buffer filtered with 0.2 μm membrane. All aqueous solutions were prepared using ≥18 MΩ ultrapure water (Milli-Q, Millipore, USA).

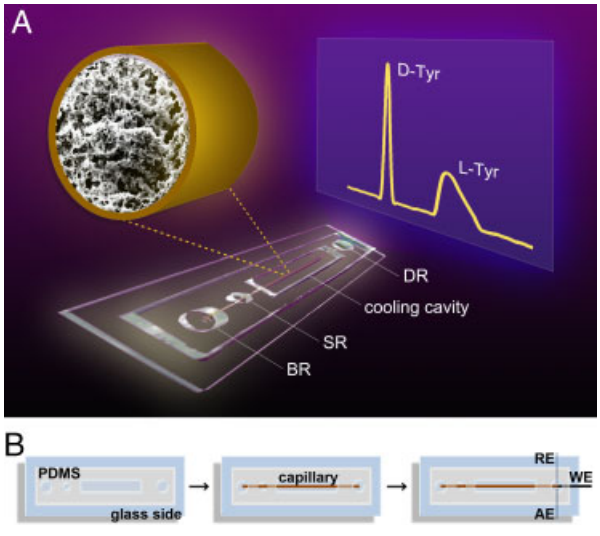

Figure 1. (A) Schematic representation of the enantioseparation on a microchip with microporous monolithic imprinted microchannel. BR, buffer reservoir; SR, sample reservoir; DR, detection reservoir. (B) Fabrication of the microchip. WE, working electrode; RE, reference electrode; AE, auxiliary electrode.

2.2 Equipments

Scanning electron micrographs (SEMs) were obtained with a Hitachi S-4800 scanning electron microscope (Japan) at an acceleration voltage of 10 kV. Fourier transform infrared (FT-IR) spectra were recorded on a Nicolet 400 FT-IR spectrometer (Madison, WI, USA). Solid-state UV–vis spectra were obtained with UV-3600 UV–vis–NIR spectrophotometer (Shimadzu, Kyoto, Japan). Ultrasonic disintegrator with a 2-mm od probe from Ningbo Scientz Biotechnology (Ningbo, China) was used to prepare the sampling fracture on the separation capillary. Microinjection pump (Baoding Longer Precision Pump, Shanghai, China) was used to operate the syringe. A laboratory-built high-voltage power supply controlled automatically by computer during experiments was used to supply separation voltage between 0 and +5000 V and sampling voltage between 0 and +1000 V, respectively. Electrochemical measurements were performed on a CHI 812 electrochemical station (CH Instruments, China). For amperometric detection, a home-made carbon fiber microdisk electrode was prepared as working electrode (WE) and the detailed description of the electrode preparation was reported elsewhere [18]. A 40 multiple microscope (Nanjing Optics Instruments Factory, Nanjing, China) was employed to monitor the position of the WE.

2.3 Preparation of monolithic superporous imprinted microchannel

Prior to preparation, a quartz capillary was flushed with 1 M NaOH followed by water for at least 30 min each. The resultant capillary was silanized by filling a mixture of 4 μL 3-(methacryloyloxy)propyltrimethoxysilane and 1 L 0.06 M acetic acid, and keeping the mixture in the capillary for 1.5 h. The silanized capillary was then flushed with water and dried with a flow of nitrogen. The composition of the prepolymerization solution is summarized in Table 1. The solution was prepolymerized by sonication for 10 min,

purged with nitrogen for 15 min to remove oxygen, and finally introduced to the capillary using a syringe. After the ends of the capillary were sealed with soft plastic rubber, the capillary was submerged in a water bath for a certain time for polymerization (Table 1). After polymerization, the capillary was flushed with ACN and methanol/acetic acid (9:1, v/v), respectively, to remove any unreacted reagent. A nonimprinted polymer (NIP)-modified capillary without template molecule was prepared with a similar process.

2.4 Fabrication of microchip

The microchip was prepared by integrating the monolithic imprinted microchannel with the PDMS matrix (13-mm width and 63-mm length) as support on a glass slide. The PDMS matrix was first prepared according our previous study [44] in which one cooling cavity and three reservoirs for buffer reservoir (BR), sample reservoir (SR), and detection reservoir (DR) were then prepared, respectively (Fig. 1A). Before integration, one small scratch was made at the position of 0.5 cm from one end of the as-prepared capillary (5.0 cm length), at which the sampling fracture was formed by an ultrasonic probe after integration. The optimal ultrasonic conditions were 150 W with an action frequency of 12 times/min and a distance of 2 mm for 1 min [44]. The WE was mounted in a guide channel of the PDMS matrix, exactly opposite to the end of the separation channel. The Ag/AgCl reference electrode and Pt wire as auxiliary electrode were inserted to the DR to obtain an integrated three-electrode system for amperometric detection (Fig. 1B). Electrodes E1, E2, E3, and E4 were inserted into SR, BR, BR, and DR to achieve the sampling and separation, respectively.

2.5 Enantioseparation of chiral compounds

The monolithic imprinted microchannel was first washed with mobile phase, which was filled in the BR and DR. The sampling voltage was applied between E1 and E2 with E3 and E4 in floating. The separation voltage was applied between E3 and E4 with E1 and E2 in floating. The fracture sampling was then performed by applying an optimum injection voltage of 200 V between the SR and the BR. The separation voltage was finally applied to the BR with the DR grounded and the SR floating by automatically switching the high-voltage contacts, and the electrochromatogram was recorded on a CHI 812 using the ''amperometric *i–t* curve'' mode. Resolution (R_s) was calculated with $R_s = 1.18(t_L - t_D)/(W_{1/2,D} + W_{1/2,L})$, where t_D and t_L are the retention times of the enantiomers, respectively, and $W_{1/2,D}$ and $W_{1/2,L}$ are the peak widths of the enantiomers at the half peak height, respectively. The microfluidic device could be renewed by cleaning the SR and sampling fracture with electrophoresis buffer.

3 Results and discussion

3.1 Preparation conditions of microporous monolithic imprinted capillary

As the selectivity and flow-through property of an imprinted monolith are very important in CEC, preparation conditions such as the polymerization temperature and time, the composition of the porogenic solvent, and the molar ratios of functional monomer to template molecule (M/T), and cross-linker to functional monomer (C/M) were first optimized (Table 1).

High temperature (70°C of capillary 5) or long time (5 h of capillary 3) would lead to low flow-through property of the monoliths (capillaries 3 and 5). When the polymerization time decreased to 4 h, the resulting capillary showed good permeability at 60°C (capillary 2). However, further decreasing temperature (50°C of capillary 4) or time of polymerization (3 h of capillary 1) led to a reduction of the number of imprinting sites and resulted in a decrease of selectivity.

Porogenic solvent also played a dual role in the morphology of the imprinted monolith such as surface area and pore size. Considering the solubility of the template, good permeability and an adequate EOF for MCEC experiments, a binary porogen consisting of ACN and isooctane was chosen [45–48]. A volume ratio (A/I) of 2:1 was found to be optimal for achieving a good template solubility and excellent permeability (capillary 2).

In addition, the molar ratios among template molecule, functional monomer, and cross-linker also affected the properties and the number of recognition sites of the MIP monolith [48, 49]. The usually used ratio of M/T is between 4:1 and 18:1 [50, 51]. When the ratio of M/T was 4:1 (capillary 2), the imprinted monolith showed the largest resolution of 2.40. The cross-linker could affect the stability and flexibility of recognition cavities, the optimal molar ratio of C/M was 10:1 (capillary 2) at which the MIP monolith showed good affinity and specific recognition toward the template L-Tyr.

Considering both the preparation time and the selectivity, the preparation conditions for capillary 2 were selected as the optimal conditions. The optimized polymerization mixture contained L-Tyr (0.025 mmol), AM (0.1 mmol), EDMA (1.0 mmol), ACN (1.2 mL), isooctane (0.6 mL), and 2,2′-azobisisobutyronitrile (6 μmol).

3.2 Characterization of microporous monolithic imprinted capillary

Figure 2A shows the SEM photograph of microporous monolith imprinted microchannel in capillary 2 (Table 1). It could be seen that the monolith had many micropores and was well linked to the inner wall of the capillary (Fig. 2B). The through-pores provided flow paths through the capillary, and the microporous network gave the monolith

Table 1. Condition optimization for the preparation of microporous monolithic imprinted microchannel[a)]

Number of capillary	A/I[b)]	Temperature (°C)	Time (h)	C/M[c)]	M/T[d)]	Permeability
1	2:1	60	3	10:1	4:1	Good
2	2:1	60	4	10:1	4:1	Good
3	2:1	60	5	10:1	4:1	Low
4	2:1	50	4	10:1	4:1	Good
5	2:1	70	4	10:1	4:1	Low
6	ACN	60	4	10:1	4:1	Low
7	8:1	60	4	10:1	4:1	Low
8	1:2	60	4	10:1	4:1	Good
9	2:1	60	4	10:1	1:1	Good
10	2:1	60	4	10:1	16:1	Good
11	2:1	60	4	2:1	4:1	Good
12	2:1	60	4	20:1	4:1	Good
13	2:1	60	4	10:1	No T	Good

a) Electrochromatographic conditions: ACN/50 mM acetate buffer (90/10, v/v, pH 4.0); detection potential, +1.2 V; injection voltage, 200 V for 2 s; separation voltage, 4000 V.
b) *A*/*I*, the volume ratio of ACN to isooctane.
c) *C*/*M*, the molar ratio of cross-linker to functional monomer.
d) *M*/*T*, the molar ratio of functional monomer to template.

a high porosity and, consequently, a good permeability. At the same time, the network of micropores was responsible for the large surface area of the monolith as well as the decrease of mass-transfer resistance from mobile phase to stationary phase. For these reasons, the microporous monolithic imprinted microchannel was efficient at high flow rates and allowed the achievement of very high efficiencies.

The effect of porogenic solvent on the morphology of the monolith was also examined by SEM. With the increase of isooctane content to A/I of 1:2 (capillary 8), the permeability became better (Fig. 2C), but the selectivity was lower than that at the ratio of 2:1 (capillary 2). At low volume content of isooctane at A/I of 8:1, the MIP skeleton became more dense and rigid, but the amount of micropores decreased (Fig. 2D), leading to low permeability (capillary 7).

To further characterize the Tyr-imprinted MIP, FT-IR spectra of the functional monomer AM, the cross-linker EDMA, MIPs before and after extraction, and NIPs were compared in Fig. 3A. The spectrum of AM showed two absorption peaks at 3356 and 3184 cm^{-1}, which were assigned to the N–H stretching vibration of the primary amide [52, 53], whereas the C = C stretching vibration occurred at 1641 cm^{-1}. The spectrum of EDMA showed a peak of C = C stretching vibration at 1637 cm^{-1}. Compared with the spectrum of AM, the spectra of MIPs both before and after extraction showed a single absorption peak at 3446 cm^{-1}, suggesting the formation of polymer [26].

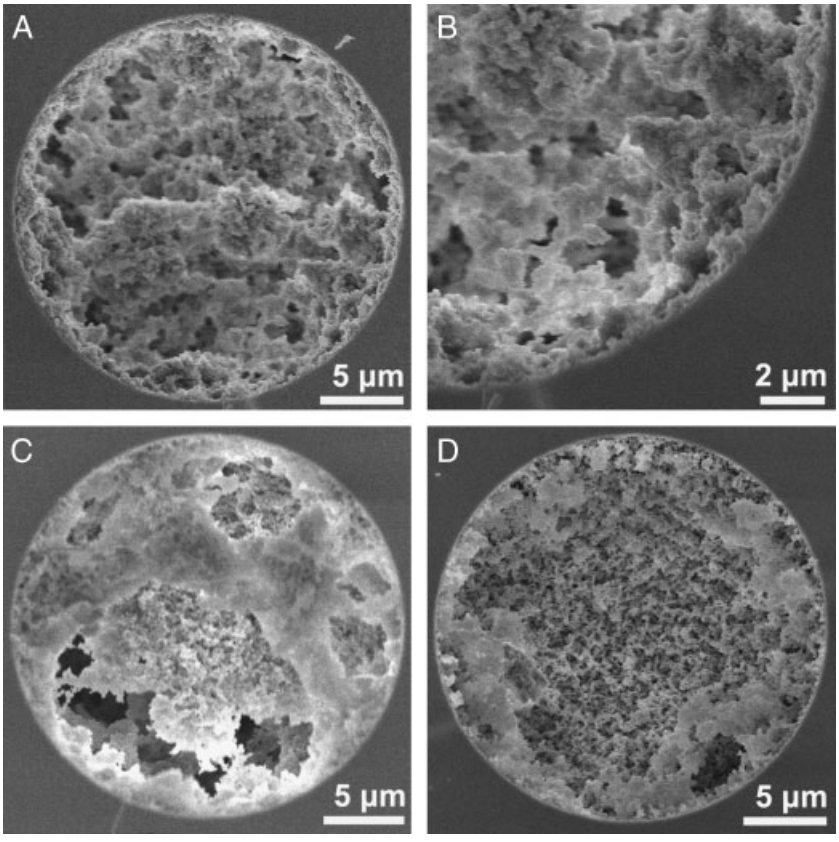

Figure 2. SEM images of microporous monolithic imprinted capillaries 2 (A and B), 7 (C), and (D) prepared at the conditions summarized in Table 1.

However, from the FT-IR spectra, it was difficult to determine whether the templates were removed after extraction because of the indistinguishable characteristics of the carbonyl stretches corresponding to the templates and the bulk polymer [54].

To confirm the removal of the template after extraction, solid-state UV–vis spectra of L-Tyr, MIPs before and after extraction, and NIPs were also compared (Fig. 3B). L-Tyr showed UV–vis absorption at 296 nm, whereas MIP before extraction showed a wide absorption band in the range from 250 to 400 nm, indicating the interactions among the templates and the specific recognition sites of MIP. The MIP after extraction showed lower UV–vis absorbance in the range from 250 to 400 nm than that before extraction, and the spectrum was similar to that of NIP, indicating the efficient removal of the templates upon extraction.

3.3 Detection potential

The electrochemical detection was employed here, which has been used in the capillary with the fracture [26, 27, 44, 55, 56]. The three-electrode system integrated with the carbon fiber microdisk electrode (WE), Ag/AgCl electrode (reference electrode), and Pt wire (auxiliary electrode). The

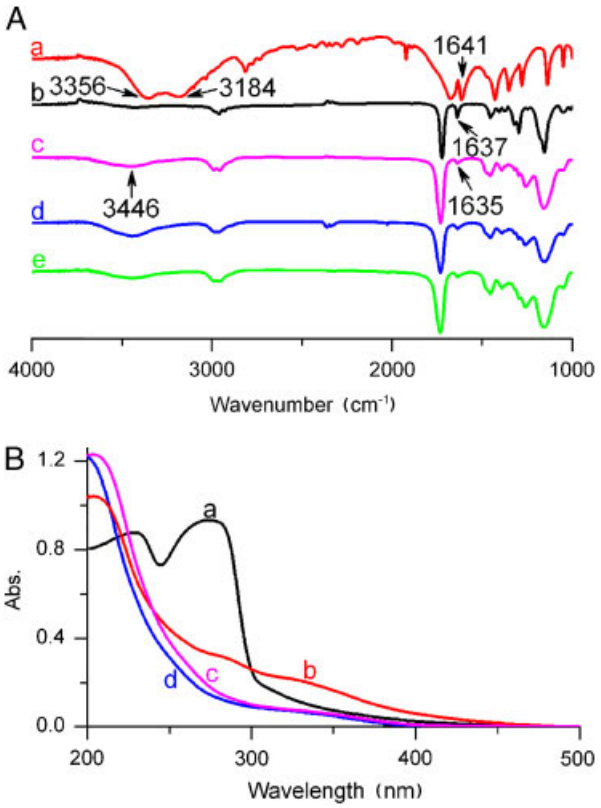

Figure 3. (A) FT-IR spectra of (a) AM, (b) EDMA, Tyr-MIP (c), before and (d) after extraction, and (e) NIP, and (B) solid-state UV–vis absorption spectra of (a) L-Tyr, Tyr-MIP (b) before and (c) after extraction, and (d) NIP.

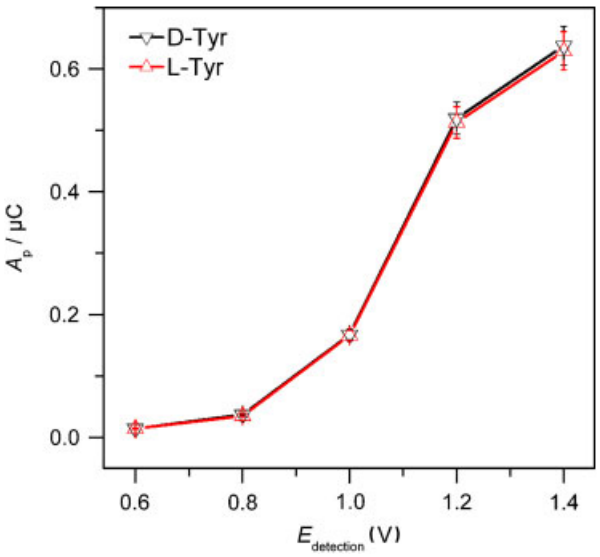

Figure 4. Effect of detection potential on peak area for 0.4 mM racemic Tyr at injection voltage of 200 V for 2 s and separation voltage of 4000 V.

electrochemical oxidation of Tyr enantiomers at the carbon fiber microdisk electrode produced detectable amperometric signal. When the applied potential was less than +0.6 V, no signal could be observed for Tyr enantiomers. With the increase of the applied potential from +0.6 to +1.2 V, the amperometric responses increased, and quick increase occurred at the potentials more positive than +1.0 V (Fig. 4). When the applied potential was higher than +1.2 V, the oxidation currents increased slowly and the baseline was unstable. Thus, +1.2 V was used as the optimum detection potential.

3.4 Optimization of chiral separation conditions

The chromatographic parameters such as the volume content of ACN, pH, and concentration of acetate buffer in mobile phase were optimized at detection potential of +1.2 V, separation voltage of 4000 V and injection voltage of 200 V for 2 s.

The effect of the volume content of ACN on the retention of Tyr enantiomers was examined at different ratios (v/v) of ACN/50 mM acetate buffer (pH 4.0) (Fig. 5A). When ACN content changed from 80 to 95%, both the retention times decreased due to the increase of the EOF [57] caused by the increase of ACN content [45]. On the other hand, a high ACN content favored imprinted molecule recognition because that ACN is a solvent with a low ability to form hydrogen bonds [47]. ACN content of 90% (v/v) in the mobile phase was used in thorough work.

The influence of pH in the range of 3.0–6.0 on the retention of Tyr enantiomers using ACN/50 mM acetate buffer (90/10, v/v) is shown in Fig. 5B. With the increase of the pH value of the mobile phase from 3.0 to 6.0, both

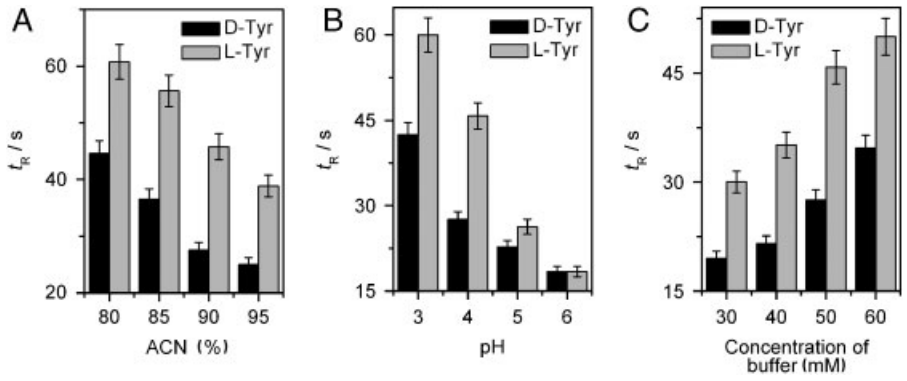

Figure 5. Effects of (A) volume content of ACN, (B) pH, and (C) concentration of acetate buffer on retention time (t_R) of D-Tyr and L-Tyr at detection potential of +1.2 V, injection voltage of 200 V for 2 s, and separation voltage of 4000 V with ACN/50 mM acetate buffer (90/10, v/v, pH 4.0) as mobile phase.

retention times decreased due to the increase of EOF. At the pH value of 5.0–6.0, the difference of retention times between D- and L-Tyr became smaller. The nonselective interactions between analytes and MIPs should be responsible for the decrease in selectivity observed at high pH value [47]. Thus, the value of pH 4.0 was selected for further optimization.

Figure 5C shows the effect of the concentration of acetate buffer (pH 4.0) mixed with ACN (10/90, v/v) on the retention of Tyr enantiomers. With the increase of the concentration, both retention times of D- and L-Tyr increased due to the decreasing EOF and elution ability. It is well known that the separation efficiency of CEC can be improved with an increasing buffer concentration. However, too high buffer concentration can cause severe Joule heating [48]. Thus, 50 mM acetate buffer was chosen to secure good separation efficiency as well as stable baseline without current disturbances.

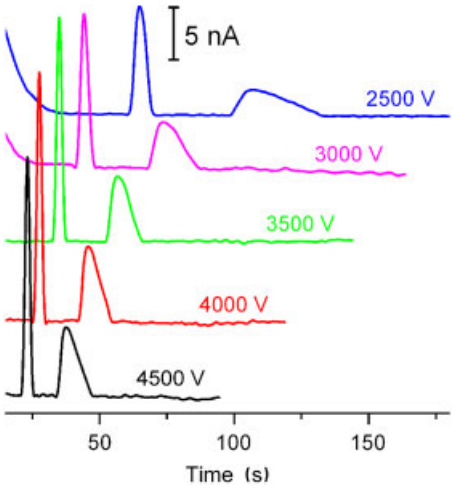

Figure 6. Effect of separation voltage on the enantioseparation of 0.4 mM racemic Tyr at detection potential of +1.2 V and injection voltage of 200 V for 2 s. Electrochromatographic conditions are the same as summarized in Table 1.

3.5 Sampling conditions and separation voltage

The designed microchip allowed injecting various volumes of sample by changing the sampling time or voltage. High sampling voltage usually results in high injection current to induce an unstable baseline and low separation efficiency. The ultranarrow sampling fracture [44] could produce a fast sampling speed at relatively low injection voltage, which allowed a short sampling time. The short time favored depressing the diffusion of the analytes during the sampling process for avoiding the broadening of the sample zone. At the sampling voltage of 200 V, with the increase of sampling time the signal increased and trended to a constant peak current after 2 s. Thus, an optimum injection voltage of 200 V at the injection time of 2 s was selected for obtaining high separation efficiency and appropriate detection sensitivity. With the increase of the separation voltage from 2500 to 4500 V, the separation time of Tyr enantiomers on the L-Tyr-imprinted microchip was greatly shortened from 135 to 48 s (Fig. 6). Meanwhile, the resolution increased from 2500 to 3500 V due to the narrow broadening of signal and then decreased at the higher separation voltages due to the too small difference between the separation times. At 4000 V, the baseline separation of Tyr enantiomers was successfully acquired with the resolution of 2.40, and the electrochromatogram showed fast separation time of 55 s and optimal peak shape without obviously tailing.

3.6 Enantioseparation of racemic Tyr

The separation efficiencies of racemic Tyr on the microchip integrated with MIP-imprinted, NIP-imprinted, and bare capillary are shown in Fig. 7. Tyr enantiomers could not be separated on both the microchip integrated with NIP- and bare capillary (electrochromatograms in Fig. 7A and B) due to the absence of recognition sites complementary to the spatial structure of Boc-L-Trp. The longer retention times on NIP-microchip resulted from the unspecific interaction between the enantiomers and the imprinted polymer. Baseline separation was achieved with the resolution

of 2.40 on the MIP-microchip (electrochromatogram in Fig. 7C), which could be attributed to sufficient recognition sites existing in the monolith imprinted capillary for the separation of Tyr.

3.7 Quantitative detection and reproducibility

Amperometric measurement was employed to detect Tyr enantiomers with a carbon fiber microdisk electrode at +1.2 V (versus Ag/AgCl). The amperometric responses increased with the increasing concentrations of racemic Tyr (Fig. 8). The linear ranges for both D-Tyr and L-Tyr were from 10 to 1200 μM with relative coefficients of 0.9998 and 0.9997, respectively (inset in Fig. 8). The detection limits at $S/N = 3$ were 2.0 and 4.0 μM for D-Tyr and L-Tyr, respectively.

The relative standard deviations (RSDs) ($n = 6$) of t_R of D-Tyr and L-Tyr were 1.2–1.4% for run-to-run, 2.3–2.4% for day-to-day, and 3.2–4.2% for chip-to-chip, respectively. The RSDs ($n = 6$) of peak areas measured at 0.4 mM racemic Tyr were 2.4316 and 2.8% for run-to-run, 4.3–5.1% for day-to-day, and 5.8–6.8% for chip-to-chip. These results suggested that the proposed method had good stability and precision, and the imprinted microchips had good fabrication reproducibility.

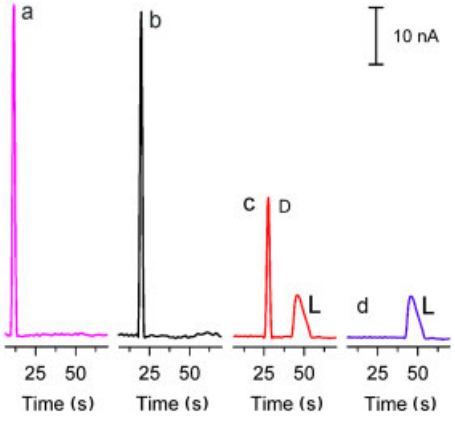

Figure 7. Electrochromatograms for enantioseparation of racemic Tyr on microchips with (A) bare, (B) NIP-imprinted, and (C) MIP-imprinted capillaries. (D) Electrochromatogram for L-Tyr on MIP-imprinted capillary. Electrochromatographic conditions are the same as summarized in Table 1.

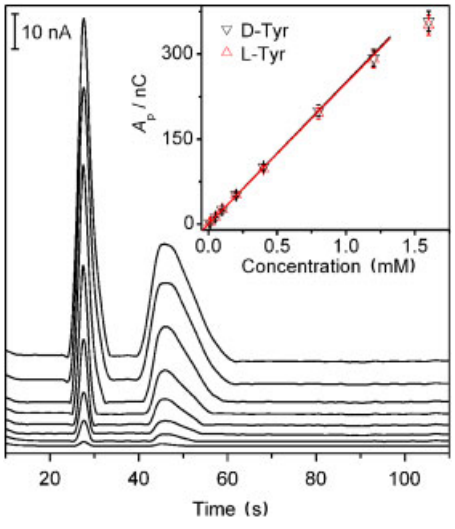

Figure 8. Electrochromatograms of racemic Tyr at 20, 100, 200, 400, 800, 1600, 2400, and 3200 μM from bottom to top. Inset: calibration curves for D-Tyr and L-Tyr detections. Electrochromatographic conditions are the same as summarized in Table 1.

4 Concluding remarks

This work fabricated a microporous monolithic imprinted microchannel for fast and sensitive chip-based enantioseparation. The microporous monolith was well linked to the inner wall of the capillary, giving a large surface area, good permeability, low mass-transfer resistance, and high efficiency. After conveniently constructing the microchip by fixing the imprinted capillary to a PDMS substrate on a glass slide, the rapid enantioseparation of racemic Tyr was achieved with good resolution and wide linear range. The designed microchip with monolithic imprinted capillary showed higher efficiency for enantioseparation versus conventional portable CE system, and opened an avenue for quick enantioscreening of chiral compounds.

The authors gratefully acknowledge the financial support of National Basic Research Program of China (2010CB732400) from the Ministry of S&T and National Natural Science Foundation of China (20821063, 20835006, 20875044).

The authors have declared no conflict of interest.

5 References

[1] Ou, J. J., Li, X., Feng, S., Dong, J., Dong, X. L., Kong, L., Ye, M. L., Zou, H. F., *Anal. Chem.* 2007, *79*, 639–646.

[2] Palmer, C. P., *Electrophoresis* 2009, *30*, 163–168.

[3] Walshe, M., Garcia, Z., Howarth, J., Smyth, M. R., Kelly, M. T., *Anal. Commun.* 1997, *34*, 119–122.

[4] Wang, H. F., Zhu, Y. Z., Yan, X. P., Gao, R. Y., Zheng, J. Y., *Adv. Mater.* 2006, *18*, 3266–3270.

[5] Huang, Y. P., Liu, Z. S., Zheng, C., Gao, R. Y., *Electrophoresis* 2009, *30*, 155–162.

[6] Jakschitz, T. A. E., Huck, C. W., Lubbad, S., Bonn, G. B., *J. Chromatogr. A* 2007, *1147*, 53–58.

[7] Cacho, C., Schweitz, L., Turiel, E., Pérez-Conde, C., *J. Chromatogr. A* 2008, *1179*, 216–223.

[8] Schweitz, L., Andersson, L. I., Nilsson, S., *Anal. Chem.* 1997, *69*, 1179–1183.

[9] Schweitz, L., *Anal. Chem.* 2002, *74*, 1192–1196.

[10] Schweitz, L., Spégel, P., Nilsson, S., *Electrophoresis* 2001, *22*, 4053–4063.

[11] Liu, J. Q., Wullf, G., *J. Am. Chem. Soc.* 2008, *130*, 8044–8054.

[12] Xu, Z. G., Hu, Y. F., Hu, Y. L., Li, G. K., *J. Chromatogr. A* 2010, *1217*, 3612–3618.

[13] Schmidt, R. H., Mosbach, K., Haupt, K., *Adv. Mater.* 2004, *16*, 719–722.

[14] Ansell, R. J., Mosbach, K., *Analyst* 1998, *123*, 1611–1616.

[15] Conrad, P. G., II , Nishimura, P. T., Aherne, D., Schwartz, B. J., Wu, D. M., Fang, N., Zhang, X., Roberts, M. J., Shea, K. J., *Adv. Mater.* 2003, *15*, 1541–1544.

[16] Hoshino, Y., Koide, H., Urakami, T., Kanazawa, H., Kodama, T., Oku, N., Shea, K. J., *J. Am. Chem. Soc.* 2010, *132*, 6644–6645.

[17] Tan, J., Wang, H. F., Yan, X. P., *Anal. Chem.* 2009, *81*, 5273–5280.

[18] González, G. P., Hernando, P. F., Alegría, J. S. D., *Biosens. Bioelectron.* 2008, *23*, 1754–1758.

[19] Henry, O. Y. F., Piletsky, S. A., Cullen, D. C., *Biosens. Bioelectron.* 2008, *23*, 1769–1775.

[20] Ou, J. J., Kong, L., Pan, C. S., Su, X. Y., Lei, X. Y., Zou, H. F., *J. Chromatogr. A* 2006, *1117*, 163–169.

[21] Wang, H. F., Zhu, Y. Z., Lin, J. P., Yan, X. P., *Electrophoresis* 2008, *29*, 952–959.

[22] Sabourin, L., Ansell, R. J., Mosbach, K., Nicholls, I. A., *Anal. Commun.* 1998, *35*, 285–287.

[23] Zaidi, S. A., Cheong, W. J., *J. Chromatogr. A* 2009, *1216*, 2947–2952.

[24] Zaidi, S. A., Cheong, W. J., *Electrophoresis* 2009, *30*, 1603–1607.

[25] Schweitz, L., Andersson, L. I., Nilsson, S., *J. Chromatogr. A* 1997, *792*, 401–409.

[26] Qu, P., Lei, J. P., Ouyang, R. Z., Ju, H. X., *Anal. Chem.* 2009, *81*, 9651–9656.

[27] Qu, P., Lei, J. P., Zhang, L., Ouyang, R. Z., Ju, H. X., *J. Chromatogr. A* 2010, *1217*, 6115–6121.

[28] Liu, H. Y., Row, K. H., Yang, G. L., *Chromatographia* 2005, *61*, 429–432.

[29] Li, H., Liu, Y., Zhang, Z., Liao, H., Nie, L., Yao, S., *J. Chromatogr. A* 2005, *1098*, 66–74.

[30] Huang, X. D., Qin, F., Chen, X. M., Liu, Y. Q., Zou, H. F., *J. Chromatogr. B* 2004, *804*, 13–18.

[31] Lin, J. M., Uchiyama, K., Hobo, T., *Chromatographia* 1998 *47*, 625–629.

[32] Chivica, G., Remcho, V. T., *Electrophoresis* 1999, *20*, 50–56.

[33] Nilsson, C., Becker, K., Harwigsson, I., Bülow, L., Birnbaum, S., Nilsson, S., *Anal. Chem.* 2009, *81*, 315–321.

[34] Schweitz, L., Spégel, P., Nilsson, S., *Analyst* 2000, *125*, 1899–1901.

[35] Svec, F., Frechet, J. M., *Anal. Chem.* 1992, *64*, 820–822.

[36] Minakuchi, H., Nakanishi, K., Soga, N., Ishizuka, N., Tanaka, N., Koyabashi, H., *Anal. Chem.* 1996, *68*, 1275–1280.

[37] Siouffi, A. M., *J. Chromatogr. A* 2003, *1000*, 801–818.

[38] Guillén-Casla, V., León-González, M. E., Pérez-Arribas, L. V., Polo-Díez, L. M., *Anal. Bioanal. Chem.* 2010, *397*, 63–75.

[39] Wolosker, H., Blackshaw, S., Snyder, S. H., *Proc. Natl. Acad. Sci. USA* 1999, *96*, 13409–13414.

[40] Nishikawa, T., *Biol. Pharm. Bull.* 2005, *28*, 1561–1565.

[41] Lapos, J. A., Manica, D. P., Ewing, A. G., *Anal. Chem.* 2002, *74*, 3348–3353.

[42] Gavin, P. F., Ewing, A. G., *Anal. Chem.* 1997, *69*, 3838–3845.

[43] Swanek, F. D., Chen, G. Y., Ewing, A. G., *Anal. Chem.* 1996, *68*, 3912–3916.

[44] Zhai, C., Qiang, W., Lei, J. P., Ju, H. X., *Electrophoresis* 2009, *30*, 1490–1496.

[45] Zheng, C., Liu, Z. S., Gao, R. Y., Zhang, L. H., Zhang, Y. K., *Anal. Bioanal. Chem.* 2007, *388*, 1137–1145.

[46] Liu, Z. S., Xu, Y. L., Yan, C., Gao, R. Y., *Anal. Chim. Acta* 2005, *523*, 243–250.

[47] Liu, Z. S., Xu, Y. L., Yan, C., Gao, R. Y., *J. Chromatogr. A* 2005, *1087*, 20–28.

[48] Deng, Q. L., Lun, Z. H., Shao, H., Yan, C., Gao, R. Y., *Anal. Bioanal. Chem.* 2005, *382*, 51–58.

[49] Tan, Z. J., Remcho, V. T., *Electrophoresis* 1998, *19*, 2055–2060.

[50] Yin, J., Yang, G. L., Chen, Y., *J. Chromatogr. A* 2005, *1090*, 68–75.

[51] Sun, B., Li, Y., Chang, W., *J. Mol. Recognit.* 2001, *14*, 388–392.

[52] Li, S. J., Huang, X., Zheng, M. X., Li, W. K., *Anal. Bioanal. Chem.* 2008, *392*, 177–185.

[53] Sunil, A. A., Tejraj, M. A., *Int. J. Pharm.* 2006, *324*, 103–115.

[54] Wang, J., Mannino, S., Camera, C., Chatrathi, M. P., Scampicchio, M., Zima, J., *J. Chromatogr. A* 2005, *1091*, 177–182.

[55] Wallingford, R. A., Ewing, A. G., *Anal. Chem.* 1987, *59*, 1762–1766.

[56] Zhai, C., Li, C., Qiang, W., Lei, J. P., Yu, X. D., Ju, H. X., *Anal. Chem.* 2007, *79*, 9427–9432.

[57] Zaidi, S. A., Han, K. M., Kim, S. S., Hwang, D. G., Cheong, W. J., *J. Sep. Sci.* 2009, *32*, 996–1001.

